HHS Public Access

Author manuscript

Chem Commun (Camb). Author manuscript; available in PMC 2019 January 18.

Published in final edited form as:

Chem Commun (Camb). 2018 January 18; 54(7): 833–836. doi:10.1039/c7cc08601f.

Fluorescence Spectroscopy Reveals N-terminal Order in Fibrillar Forms of α-Synuclein

Conor M. Haney[a] and **E. James Petersson**[a]

[a]Department of Chemistry, University of Pennsylvania, 213 South 34th Street, Philadelphia, PA 19104, USA. ejpetersson@sas.upenn.edu; Tel: +1-215-746-2221

Abstract

The neuronal protein α-synuclein (αS) plays a key role in Parkinson's Disease, forming inclusions termed Lewy Bodies and Lewy Neurites. Recent improvements in cryo-electron diffraction and solid state NMR (ssNMR) have led to the elucidation of the structures of peptides derived from the αS fibril core and full-length human αS in fibrils. Despite the valuable insight offered by these methods, there are still several questions about the structures' relevance to pathological aggregates. Herein, we present fluorescence data collected *in vitro* under the conditions which fibrils are typically assembled. Our data suggest that, in solution, fibrils are largely structured as observed by ssNMR. However, we observe significant disparities in the αS N-terminus as compared to ssNMR data, which provide insight on its important role in αS aggregation and fibril structure.

The intrinsically disordered protein α-synuclein (αS) is associated with the etiology of a number of diseases collectively known as synucleinopathies, of which the most common is Parkinson's Disease (PD).[1] Physiologically, αS is believed to play a role in vesicle trafficking and neurotransmitter release.[2] In PD, αS is found in intracellular inclusions termed Lewy Bodies and Lewy Neurites.[3] The presence of these aggregates correlates with the loss of dopaminergic neurons in the substantia nigra pars compacta.[4, 5] The loss of dopaminergic neurons leads to progressive neurodegeneration and clinical symptoms including resting tremor, rigidity, and bradykinesia.

Since the discovery that αS is implicated in PD and related synucleinopathies, significant effort has been devoted to understanding the formation of aggregates, as well as their structure and role in disease progression.[3, 6] Traditionally, structural investigations of αS fibrils have been limited by the intractability of structural methods such as X-ray crystallography or solution NMR in elucidating fibril structures. Recently, cryo-electron diffraction (ED) has been applied to elucidate the packing interactions between short peptide fragments derived from the αS non-amyloid component (NAC) domain, which forms the fibril core.[7] Advances in solid-state NMR (ssNMR) have now enabled structural characterization of full-length human wild-type (WT) αS within a fibril.[8] Despite the insight offered by these structural methods, there remains some doubt about their direct relevance to

Conflicts of interest

There are no conflicts to declare.

the aggregates formed *in vitro* under the conditions of most biochemistry experiments. Furthermore, these structural techniques have been unable to elucidate the role of the N- and C-terminal regions of αS in fibrils. While these regions are presumed to be highly dynamic and unstructured based on ssNMR and hydrogen-deuterium exchange experiments, alternate lines of evidence suggest a role for the termini in modulating aggregation driven by the NAC domain.[8–10] Additionally, several studies have shown that N-terminal regions of αS remain inaccessible to proteolytic degradation in fibrils, suggesting that this region is inaccessible and may be partly structured.[11, 12] Several small molecules have been shown to interact with the N-terminal portion of αS and modulate its fibrillization, suggesting an important role for this protein region in modulating aggregation.[13, 14]

Here, we apply a variety of fluorescence spectroscopy techniques to investigate the structure of αS fibrils. We find that the parallel, in-register packing of individual chains observed in the ssNMR structure is largely consistent with our observations about the mode of interchain association. Our measurements agree that the fibril core, or NAC, is the most highly structured portion of the protein, while the C-terminus remains dynamic. However, the N-terminal residues of αS fibrils appear to be more closely associated with the core than previously thought.

We began our investigations by employing labeling positions within the αS sequence previously determined to be non-disruptive to aggregation.[15, 16] We used unnatural amino acid (Uaa) mutagenesis to introduce a propargyltyrosine (PpY) residue which was subsequently labeled via copper (I) catalyzed azide-alkyne cycloaddition (CuAAC) to install a tetramethylrhodamine (Tmr) fluorophore (Fig. 1).[17] We have optimized methods for the expression, purification, and labeling of singly- and doubly-labeled αS, providing ~1 mg of labeled material within one week. Similar to prior work undertaken in our lab, we then extensively characterized each singly-labeled species by measurement of aggregation kinetics, circular dichroism (CD) spectra in the presence of sodium dodecyl sulfate (SDS) and examination of the aggregates via transmission electron microscopy (TEM).[15, 16] In each case, the labeled protein exhibited a half-time of aggregation ($t_{1/2}$) similar to that of WT protein, and the resulting aggregates were morphologically indistinguishable from WT αS fibrils (see ESI, Fig. S6, Fig. S21). We next utilized our pre-existing library of αS mutants with cysteine residues dispersed throughout the sequence. Each αS-Cys protein was expressed, purified, and labeled with pyrene-1-maleimide (Pyr), a useful fluorophore which exhibits excimer formation upon Pyr/Pyr contact in the excited state (see ESI, Fig. S8).[18] Following generation of the αS-Cys^{Pyr}_{X} (X denotes the sequence position) library, we undertook a series of experiments designed to examine the intermolecular association of monomer units within αS fibrils. In each aggregation, αS-Cys^{Pyr}_{X} comprised 25 mol % of the monomer pool, with the remainder being unlabeled WT αS. Fluorescence spectra were acquired at the beginning and end of aggregation and for the resuspended fibrils. As expected, positions within or proximal to the NAC domain (e.g., 42, 62, 87) exhibited strong excimer fluorescence with emission from 475–485 nm (Fig. 2A). Surprisingly, N-terminal positions (9, 24) also exhibited a moderate degree of excimer fluorescence. The C-terminal positions (114, 123, 136) lacked evidence of excimer formation (Fig. 2A). In no case did we observe excimer fluorescence from monomeric αS (see ESI, Fig. S8). For all of the positions studied, inclusion of labeled protein perturbed neither the incorporation of αS into

fibrils nor the morphology of the aggregates observed by TEM. (see ESI, Fig. S20, S21). Our results utilizing eight different αS-C^{Pyr}_X variants demonstrate a parallel, in-register packing of monomer units within αS fibrils. Furthermore, excimer fluorescence is observed at core positions within the sequence, consistent with intermolecular packing within the NAC domain observed from ssNMR. Remarkably, we also observe excimer fluorescence from N-terminally labeled positions, suggestive of appreciable intermolecular N-terminal contacts not previously observed. However, it has long been appreciated that distal portions of αS may play a role in aggregation, and that the N-terminus in particular may be more ordered than many structural methods have been capable of capturing.[9, 10, 19, 20]

To further understand these apparent differences in dynamics compared to the ssNMR structure, we undertook experiments using fluorescein (Fam) labeled protein, αS-C^{Fam}_X, and the established photoinduced electron transfer (PET) quencher, thioacetamide.[21, 22] Fibrils were prepared containing 1 mol % of each of the αS-C^{Fam}_X (indicating αS with cysteine-fluorescein conjugate at position X) proteins and resuspended in buffer containing either 0 or 100 mM thioacetamide. Collection of steady-state spectra revealed robust thioamide-induced PET quenching of fluorescein fluorescence throughout the αS sequence in monomer with significant decreases in quenching efficiency for the same positions in fibrils (Fig. S10). Time-correlated single photon counting (TCSPC) distributions suggest that there are at least two conformational populations for the C-terminus, consisting of high and low quenching states (Fig. S11). Prior studies by Sahay *et al.* used Trp quenching by acrylamide to show that N-terminal positions are more accessible than internal positions, though less accessibe than C-terminal positions.[23] However, a comparison to monomeric protein was not made in that work, so the differences with our observations may be the result of differences in the intrinsic reactivity of our probes. It is also possible that the larger size and longer linker of C^{Fam} may be somewhat disruptive to local structure, in spite of our validation efforts.

Having established robust methods for generating doubly-labeled αS containing a Fam donor fluorophore and tetramethylrhodamine (Tmr) acceptor fluorophore, a Förster resonance energy transfer (FRET) pair with a distance of half-maximal energy transfer of ~55 Å[24], we generated a moderate-size doubly-labeled library of αS mutants. As above, the labeling positions are indicated by a subscript and the fluorophore by a superscript, e.g. αS-C^{Fam}_XPpY$^{Tmr}_Y$ indicating αS with cysteine-fluorescein conjugate at position X and propargyltyrosine-tetramethylrhodamine conjugate at position Y. In each case, doubly-labeled protein was utilized at 1 mol % of the monomer pool in order to prevent intermolecular fluorophore cross-talk. Aggregation of the labeled protein was shown to be non-perturbing for each of these positions, as demonstrated previously or herein.[15, 16] Surprisingly, we observed a significant bathochromic shift in the spectra of fluorescein-labeled proteins in fibrils relative to monomer, suggestive of the fluorophore being sequestered in an environment of diminished hydrogen bonding upon fibril formation (Fig. S12).[25, 26] This point underscores the importance of collecting spectra of singly-labeled proteins for spectral deconvolution of the doubly-labeled species (see ESI, Fig. S16). We collected steady-state and time correlated single photon counting (TCSPC) spectra at the start and end of aggregation and on resuspended fibrils in triplicate. We then deconvoluted

the doubly-labeled spectra and fit TCSPC decays to exponential functions in order to determine the FRET efficiency, E_{FRET}, for intramolecular distance determination.

Our measurements using fluorophore pairs within or proximal to the NAC domain (e.g. αS-$C^{Fam}_{42}PpY^{Tmr}_{94}$, αS-$C^{Fam}_{87}PpY^{Tmr}_{35}$) were largely consistent with the C_β-C_β intramolecular distances extracted from the ssNMR structure (PDB: 20NA; Fig. 3, ESI Table S4, Fig. S16).[8] Deviations in the most tightly-packed regions of the fibril core may be attributable to the fluorophore linker (ESI Table S4, Fig. S16). In contrast, intramolecular distances obtained from N-terminal donor positions (αS-$C^{Fam}_{9}PpY^{Tmr}_{94}$, αS-$C^{Fam}_{24}PpY^{Tmr}_{94}$) and N-to-C terminal distances (αS-$C^{Fam}_{9}PpY^{Tmr}_{136}$) were shorter than expected. It is possible that the less structured regions of the protein are more appropriately treated using polymer-scaled distance distributions often applied to intrinsically disordered proteins.[27–29] In light of this, we have applied polymer scaling methods to the monomeric protein FRET measurements, as well as for αS-$C^{Fam}_{9}PpY^{Tmr}_{136}$ in fibrils, as prior methods have suggested that this FRET pair may behave similar to a polymer due to disorder at the termini.

Taken together with the pyrene data, this is suggestive of a fibril conformation in which the N-terminal portion of αS folds back towards the NAC. Overall, our data suggest a more collapsed conformation for both termini than the ssNMR model wherein the termini are unstructured and directed away from the NAC domain. Incorporation of only 1% labeled protein rules out the possibility of these distances being artifactually derived from intermolecular fluorophore cross-talk. Notably, our data acquisition was performed on fibrils suspended in buffer, representing the first solution-phase measurements of intramolecular conformations in αS fibrils. It is possible that the differences we observe from prior models are due, in part, to the requirement that prior data be collected in the solid state or under cryogenic conditions. Importantly, cryogenic treatment or storage of αS fibrils has previously been shown to alter fibril structure, suggesting these methods may not be ideal for representation of fibrils, particularly more flexible regions like the termini.[30] Indeed, a subset of our constructs exhibited changes in FRET efficiency or excimer fluorescence following cryogenic freezing and thawing (Fig. S18, Table S6).

Our FRET results are largely consistent with the ssNMR structure within the core. Unfortunately, cryo-ED derived structures of peptides derived from the fibril core are too small to serve as a direct point of comparison, other than consistency with pyrene excimer results.[7] However, the models built by assembling the high resolution cryo-ED fragment structures clearly disagree with our data as well as the ssNMR structure. The ssNMR structure as well as prior models of αS in fibrils include a larger end-to-end distance than is evident from our measurements, even when the termini are treated with polymer-scaled FRET distributions. This conformational model is consistent with the N-terminus orienting back towards the NAC domain, and the C-terminus potentially orienting towards the C-terminal portion of the NAC.

A recent study employing molecular dynamics (MD) simulations of models of αS fibrils has suggested a close contact between N- and C-termini in fibrillar structures.[31] Interestingly, the structures in which this contact was present were found to be of similar stability to the

structures observed by ssNMR on the timeline used in simulations, which has important implications for the potential for fibril polymorphisms of αS. However, the models generated by MD were derived based on biased inclusion of N- and C-terminal contacts in starting structures. While we observe that the termini approach the NAC more closely than exhibited by the ssNMR model, the MD model is much too compacted and inconsistent with our measurements.

We can generate our own structural model by simply identifying the N- and C-terminal conformations within the 10 αS monomer structures in the ssNMR data that are most consistent with our measurements. A merged structure containing the common core conformation (residues 35–94) and these optimal termini is shown in Figure 3. This is a crude model, but it does allow one to begin generating testable hypotheses regarding the effects of mutations in the termini. For example, the A30P mutation associated with familial PD may cause the N-terminus to fold back as in our model, leading to a more aggregation-prone monomeric conformation or alternations to fibril packing.[32] To generate a more rigorous atomistic αS fibril model, we are currently pursuing experimentally-constrained Monte Carlo (ECMC) simulations using fluorescence data. We and others have recently used similar ECMC modeling to study the conformational ensemble of αS monomers.[33, 34]

Conclusions

In conclusion, here we have applied an array of fluorescence spectroscopic methods to investigate the fibrillar structure of the PD-associated protein αS under conditions which fibrils are typically prepared. Our measurements reflect an in-register, parallel conformation of monomers within fibrils in which the N-terminus forms intermolecular contacts, while the C-terminus remains disordered. Intramolecular distances derived using FRET are consistent with the ssNMR model of the fibril core, but differ in that the N- and C-termini fold back towards the fibril core. Notably, our observations regarding the N-terminal portion of αS are consistent with a recently reported fibril polymorph of αS, in which the N-terminus is resistant to hydrogen-deuterium exchange, suggesting ordering of the N-terminal region.[35] Overall, our data support the majority of the structural information available on αS fibrils, but point to important contributions of N-terminal regions on αS fibril formation and structure. With effective means of studying αS fibril structures *in situ*, we are now applying these tools to understanding how small molecules may modulate fibril structures by detection of intramolecular rearrangements following treatment. Furthermore, several fibril isoforms or strains of αS have been reported, but as yet it is unclear how these strains differ structurally.[36] Our fluorescent tools offer a facile means of structurally differentiating these species under near physiological conditions, which will facilitate development of specific means of targeting particular strains exhibiting variable pathology in disease models.

Supplementary Material

Refer to Web version on PubMed Central for supplementary material.

Acknowledgments

This work was supported by funding from the University of Pennsylvania, as well as grants from the National Institutes of Health (NIH NS081033 to EJP). Instruments supported by the National Science Foundation include: MALDI MS (NSF MRI-0820996) and CD (NSF DMR05-20020). CMH was supported by an Age Related Neurodegenerative Disease Training Grant fellowship (NIH T32AG000255).

Notes and references

1. Theillet F-X, Binolfi A, Bekei B, Martorana A, Rose HM, Stuiver M, Verzini S, Lorenz D, van Rossum M, Goldfarb D. Nature. 2016; 530:45. [PubMed: 26808899]
2. Bendor JT, Logan Tp Fau - Edwards RH, Edwards RH. Neuron. 2013:1044–1066. [PubMed: 24050397]
3. Spillantini M S, L M, Lee VM, Trojanowski JQ, Jakes R, Goedert M. Nature. 1997
4. Bourdenx M, Koulakiotis NS, Sanoudou D, Bezard E, Dehay B, Tsarbopoulos A. Prog. Neurobiology. 2017; 155:171–193.
5. Brettschneider J, Del Tredici K, Lee VM, Trojanowski JQ. Nat. Rev. Neurosci. 2015:109–120. [PubMed: 25588378]
6. Polymeropoulos MH, Lavedan C, Leroy E, Ide SE, Dehejia A, Dutra A, Pike B, Root H, Rubenstein J, Boyer R, Stenroos ES, Chandrasekharappa S, Athanassiadou A, Papapetropoulos T, Johnson WG, Lazzarini AM, Duvoisin RC, Di Iorio G, Golbe LI, Nussbaum RL. Science. 1997; 276:2045. [PubMed: 9197268]
7. Rodriguez JA, Ivanova MI, Sawaya MR, Cascio D, Reyes FE, Shi D, Sangwan S, Guenther EL, Johnson LM, Zhang M, Jiang L, Arbing MA, Nannenga BL, Hattne J, Whitelegge J, Brewster AS, Messerschmidt M, Boutet S, Sauter NK, Gonen T, Eisenberg DS. Nature. 2015; 525:486–490. [PubMed: 26352473]
8. Tuttle MD, Comellas G, Nieuwkoop AJ, Covell DJ, Berthold DA, Kloepper KD, Courtney JM, Kim JK, Barclay AM, Kendall A, Wan W, Stubbs G, Schwieters CD, Lee VMY, George JM, Rienstra CM. Nat Struct Mol Biol. 2016; 23:409–415. [PubMed: 27018801]
9. Lucato CM, Lupton CJ, Halls ML, Ellisdon AM. J. Mol. Biol. 2017; 429:1289–1304. [PubMed: 28342736]
10. Del Mar C, Greenbaum EA, Mayne L, Englander SW, Woods VL. Proc. Nat. Acad. Sci. USA. 2005; 102:15477–15482. [PubMed: 16223878]
11. Zhang Z, Kang SS, Liu X, Ahn EH, Zhang Z, He L, Iuvone PM, Duong DM, Seyfried NT, Benskey MJ, Manfredsson FP, Jin L, Sun YE, Wang J-Z, Ye K. Nat Struct Mol Biol. 2017; 24:632–642. [PubMed: 28671665]
12. McGlinchey RP, Dominah GA, Lee JC. Biochemistry. 2017; 56:3881–3884. [PubMed: 28614652]
13. Rao JN, Dua V, Ulmer TS. Biochemistry. 2008; 47:4651–4656. [PubMed: 18366183]
14. Lendel C, Bertoncini CW, Cremades N, Waudby CA, Vendruscolo M, Dobson CM, Schenk D, Christodoulou J, Toth G. Biochemistry. 2009; 48:8322–8334. [PubMed: 19645507]
15. Haney CM, Wissner RF, Warner JB, Wang YJ, Ferrie JJ, Covell DJ, Karpowicz RJ, Lee VMY, James Petersson E. Org. Biomol. Chem. 2016; 14:1584–1592. [PubMed: 26695131]
16. Haney CM, Cleveland CL, Wissner RF, Owei L, Robustelli J, Daniels MJ, Canyurt M, Rodriguez P, Ischiropoulos H, Baumgart T, Petersson EJ. Biochemistry. 2017; 56:683–691. [PubMed: 28045494]
17. Deiters A, Schultz PG. Bioorg. Med. Chem. Lett. 2005; 15:1521–1524. [PubMed: 15713420]
18. Thirunavukkuarasu S, Jares-Erijman EA, Jovin TM. J. Mol. Biol. 2008; 378:1064–1073. [PubMed: 18433772]
19. Der-Sarkissian A, Jao CC, Chen J, Langen R. J. Biol. Chem. 2003; 278:37530–37535. [PubMed: 12815044]
20. Comellas G, Lemkau LR, Nieuwkoop AJ, Kloepper KD, Ladror DT, Ebisu R, Woods WS, Lipton AS, George JM, Rienstra CM. J. Mol. Biol. 2011; 411:881–895. [PubMed: 21718702]
21. Goldberg JM, Batjargal S, Chen BS, Petersson EJ. J. Am. Chem. Soc. 2013; 135:18651–18658. [PubMed: 24266520]

22. Petersson EJ, Goldberg JM, Wissner RF. Phys. Chem. Chem. Phys. 2014; 16:6827–6837. [PubMed: 24598971]
23. Sahay S, Anoop A, Krishnamoorthy G, Maji SK. Biochemistry. 2014; 53:807–809. [PubMed: 24450731]
24. Merzlyakov, M., Hristova, K. Meth. Enzymology. Vol. 450. Academic Press; 2008. p. 107-127.
25. Klonis N, Clayton AHA, Voss EW, Sawyer WH. Photochem. Photobiol. 1998; 67:500–510. [PubMed: 9613235]
26. Naderi F, Farajtabar A. J. Mol. Liq. 2016; 221:102–107.
27. McNulty BC, Tripathy A, Young GB, Charlton LM, Orans J, Pielak GJ. Protein Sci. 2006; 15:602–608. [PubMed: 16452621]
28. Ferreon ACM, Moosa MM, Gambin Y, Deniz AA. Proc. Nat. Acad. Sci. USA. 2012; 109:17826–17831. [PubMed: 22826265]
29. Schuler B, Soranno A, Hofmann H, Nettels D. Annu. Rev. Biophys. 2016; 45:207–231. [PubMed: 27145874]
30. Ikenoue T, Lee Y-H, Kardos J, Saiki M, Yagi H, Kawata Y, Goto Y. Angew. Chemie Int. Ed. 2014; 53:7799–7804.
31. Bloch DN, Miller Y. ACS Omega. 2017; 2:3363–3370.
32. Nielsen SB, Macchi F, Raccosta S, Langkilde AE, Giehm L, Kyrsting A, Svane ASP, Manno M, Christiansen G, Nielsen NC, Oddershede L, Vestergaard B, Otzen DE. PLOS ONE. 2013; 8:e67713. [PubMed: 23861789]
33. Nath A, Sammalkorpi M, DeWitt David C, Trexler Adam J, Elbaum-Garfinkle S, O'Hern Corey S, Rhoades E. Biophys. J. 2012; 103:1940–1949. [PubMed: 23199922]
34. Ferrie JJ, Haney CM, Yoon J, Pan B, Fakhraai Z, Rhoades E, Nath A, Petersson EJ. Biophys. J. Accepted Manuscript.
35. Kumar H, Singh J, Kumari P, Udgaonkar JB. J. Biol. Chem. 2017; 292:16891–16903. [PubMed: 28760825]
36. Peelaerts W, Baekelandt V. J. Nerochem. 2016; 139:256–274.

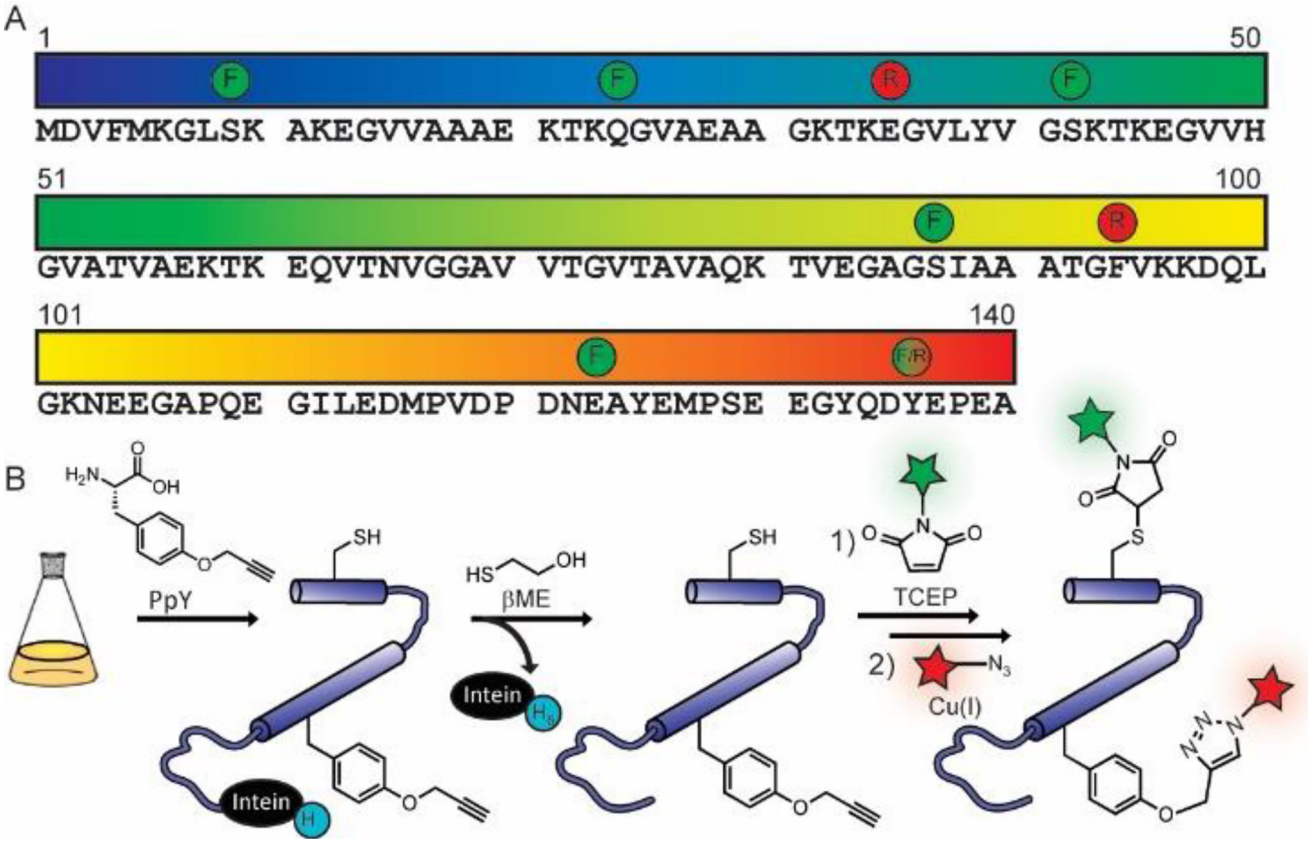

Fig. 1.

αS Sequence and Labeling. (A) αS sequence with labeling positions highlighted for locations chosen for fluorescein (Fam, green) or rhodamine (Tmr, red) labeling. Fam positions were also used for labeling with pyrene-1-maleimide (Pyr). (B) Production of doubly-labeled αS.

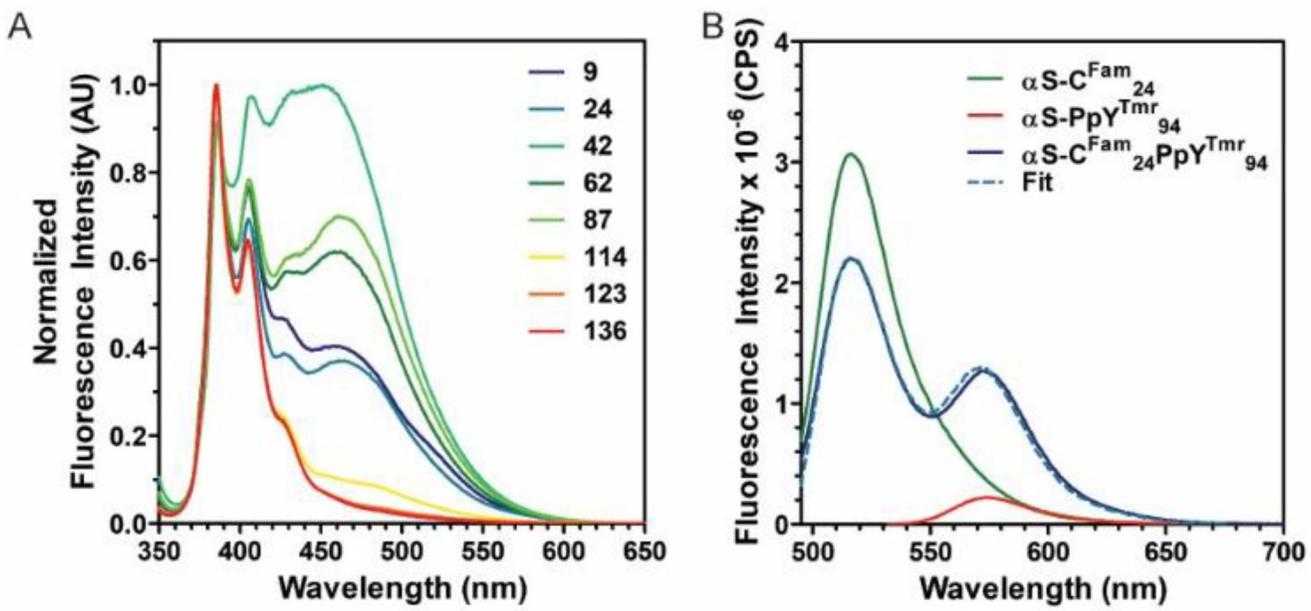

Fig. 2.

Fluorescence in αS Fibrils. (A) Normalized fluorescence emission spectra for αS-C^{Pyr}_{X} fibrils. (B) Emission spectra for resuspended fibrils containing 1% αS-C^{Fam}_{24} (green), αS-PpY^{Tmr}_{94} (red) and αS-$C^{Fam}_{24}PpY^{Tmr}_{94}$ (blue) with the fit (dashed light blue) used to extract intramolecular distances as described in ESI.

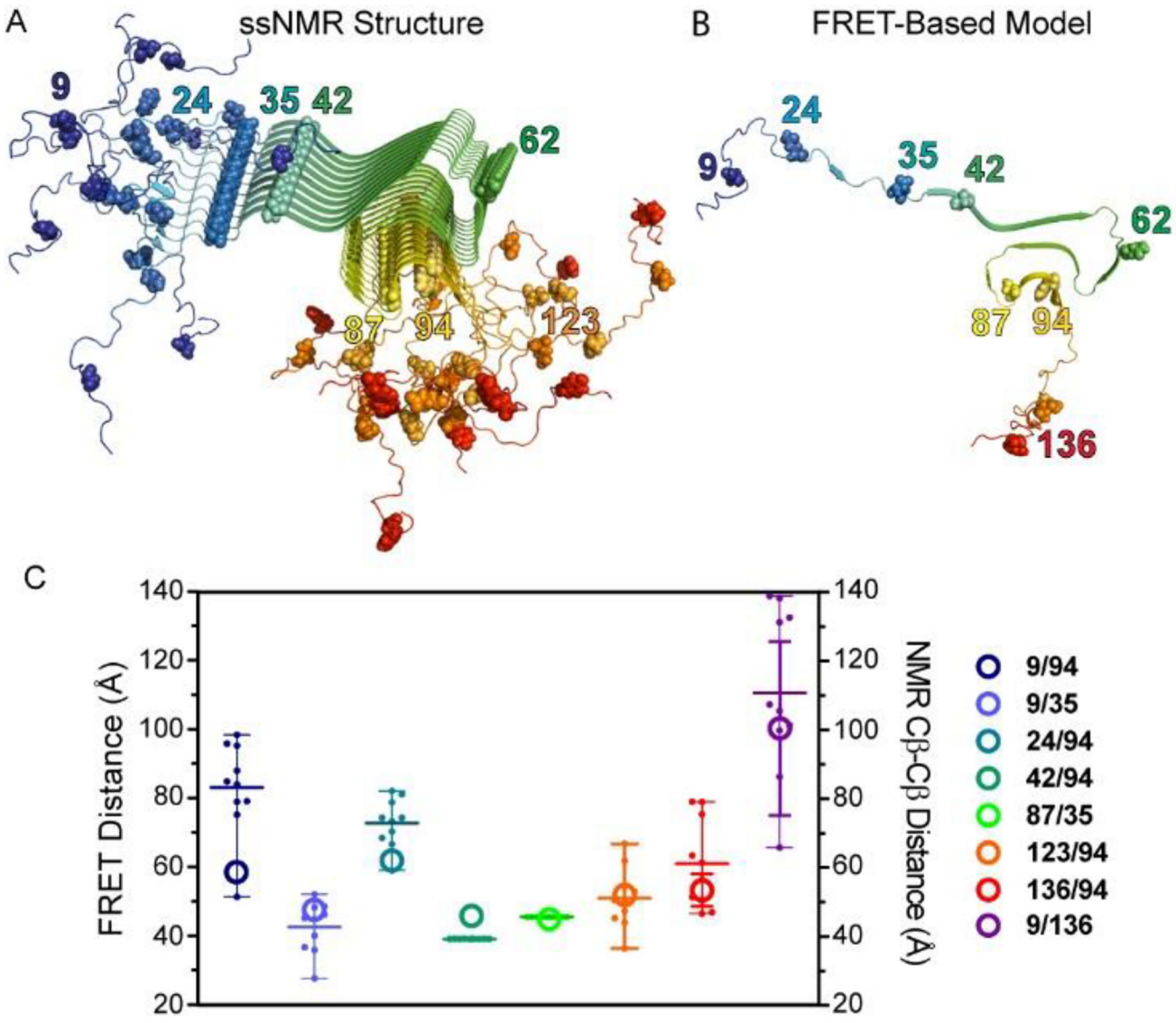

Fig. 3.

Comparison of FRET and ssNMR distances. (A) ssNMR structure (PDB: 20NA) with labeling positions used highlighted as spheres and color coded from N-terminus (blue) to C-terminus (red). (B) Extracted model of the fibril structure which best matches intramolecular FRET data. (C) Overlay of FRET distances (left Y-axis, open circles and thick error bars; mean and standard deviation) and ssNMR derived Cβ-Cβ distances (right Y-axis, dots; plotted as the mean and range).